Electrochimica Acta 142 (2014) 261–267

Contents lists available at ScienceDirect

Electrochimica Acta

journal homepage: www.elsevier.com/locate/electacta

Photovoltaic performance of dye-sensitized solar cells assembled with electrospun polyacrylonitrile/silica-based fibrous composite membranes

Jinxing Zhao, Sung-Geun Jo, Dong-Won Kim *

Department of Chemical Engineering, Hanyang University, Seungdong-Gu, Seoul 133-791, Republic of Korea

ARTICLE INFO

Article history:
Received 3 April 2014
Received in revised form 24 June 2014
Accepted 28 July 2014
Available online 12 August 2014

Keywords:
Dye-sensitized solar cell
Electrochemical characteristics
Fibrous composite membrane
Ionic conductivity
Photovoltaic performance

ABSTRACT

Electrospun fibrous composite membranes composed of polyacrylonitrile (PAN) and silica nanoparticles are prepared with different proportions of SiO_2. The membranes have three-dimensional and fully interconnected network structures in which the SiO_2 nanoparticles are homogeneously distributed. The PAN/SiO_2 fibrous composite membranes encapsulate a large amount of liquid electrolyte and exhibit high ionic conductivities. The electrochemical characteristics of dye-sensitized solar cells (DSSCs) are dependent on the content of SiO_2 nanoparticles in the fibrous composite membranes. We demonstrate that DSSC assembled with a PAN/SiO_2 fibrous composite membrane containing 10 wt.% SiO_2 exhibits the remarkably high conversion efficiency of 7.85% at 100 mW cm^{-2}, as well as better long-term stability than a DSSC with liquid electrolyte.

1. Introduction

Dye-sensitized solar cells (DSSCs) have attracted great attention because of their low production cost, easy fabrication and relatively high conversion efficiency [1,2]. A high conversion efficiency of 12% has been achieved in a DSSC with an organic liquid electrolyte [3]. However, leakage or evaporation of liquid electrolytes from DSSCs has been a critical problem that limits their long-term operation and practical application [4]. In order to improve the long-tem stability of DSSCs, a lot of attempts have been made to replace liquid electrolytes with gel polymer electrolytes that exhibit high ionic conductivity and improved stability [5–9]. Gel polymer electrolytes are usually prepared by incorporating liquid electrolyte into a matrix polymer; examples include poly(ethylene oxide) (PEO), polyacrylonitrile (PAN), poly(vinylidene fluoride) (PVdF), poly(vinylidene fluoride-co-hexafluoropropylene) (PVdF-HFP) and poly(methyl methacrylate) (PMMA), and their ionic conductivities usually exceed 10^{-3} S cm^{-1} at room temperature [10]. However, such gel polymer electrolytes suffer from poor mechanical strength, making assembly difficult and also the impregnation of liquid electrolyte into a polar polymer results in softening of the polymer, increasing the incidence of shorting between electrodes. To overcome these problems, an activation process in which a porous polymer membrane is soaked in an electrolyte solution has been investigated for DSSC applications [11–16]. Unlike conventional methods such as solution casting and direct dissolution of the polymer in the electrolyte solution, this procedure handles the mechanically robust porous membrane until adding liquid electrolyte to it at last. To prepare the porous polymer membrane, many techniques have been used, such as drawing, template synthesis, phase inversion and electrospinning [17–23]. Among these, the electrospinning technology is a simple and low-cost method for making a highly porous membrane with nanofibers. It has been reported that electrospun membranes based on PVdF-HFP effectively encapsulated the organic solvent containing I^-/I_3^- redox couple and promoted a strong interfacial contact between the dye-adsorbed TiO_2 electrode and the Pt counter electrode [12–15]. PAN is also a polymer material that can be used in preparing gel polymer electrolytes exhibiting high ionic conductivity, thermal stability and good compatibility with organic solvents [11,24–28]. However, there are few reports about the preparation and characterization of PAN-based electrospun fibrous polymer membranes for DSSC applications. It has been well demonstrated that the incorporation of ceramic fillers such as SiO_2, Al_2O_3, and TiO_2 to form the composite polymer electrolytes could improve their mechanical strength and ionic conductivity [29]. Thus, it is of great interest to use the electrospun PAN-based fibrous composite membrane as a polymer electrolyte in a quasi-solid-state DSSC. In this study,

* Corresponding author. Tel.: +82 2 2220 2337; fax: +82 2 2298 4101.
E-mail address: dongwonkim@hanyang.ac.kr (D.-W. Kim).

http://dx.doi.org/10.1016/j.electacta.2014.07.109
0013-4686/

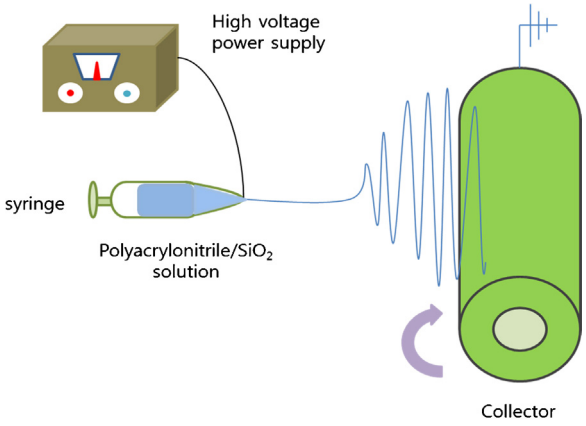

Fig. 1. Schematic representation of the electrospinning technique used to prepare fibrous PAN and PAN/SiO_2 composite membranes.

electrospun PAN/silica-based fibrous composite membranes containing different content of SiO_2 nanoparticles are prepared and their electrochemical characteristics are investigated. DSSCs employing the electrospun PAN/SiO_2 fibrous composite membranes are fabricated, and their photovoltaic performance is evaluated and compared to that of a cell containing liquid electrolyte. To our best knowledge, this is the first reported attempt to assemble and evaluate the performance of DSSCs that incorporate the electrospun PAN/SiO_2-based fibrous composite membranes.

2. Experimental

2.1. Materials

PAN (Mw =150,000), acetonitrile, N,N-dimethylformamide (DMF), chloroplatinic acid hydrate, 4-tert-butylpyridine (TBP), lithium iodide and iodine were purchased from Sigma-Aldrich. Fumed silica (TS530) was supplied by CABOT. Nanocrystalline TiO_2 paste (Ti-Nanoxide T20/SP), *cis*-diisothiocyanato-bis(2,2′-bipyridyl-4,4′-dicarboxylato) ruthenium (II) bis(tetrabutyl ammonium) (Ruthenium 535 bis-TBA, N719) and hot melting film (Surlyn, SX1170) were purchased from Solaronix. Fluorine-doped tin oxide glass was purchased from Pilkington. All commercial reagents were used as received.

2.2. Preparation of electrospun PAN and PAN/SiO_2 fibrous membranes

The electrospun PAN and PAN/SiO_2 fibrous composite membranes were prepared by an electrospinning method (Fig. 1) as follows. PAN was dissolved in anhydrous DMF at 60 °C to a concentration of 10 wt.%. Different amounts of fumed silica (0, 5, 10, 15, 20 wt.% relative to PAN) were added to the polymer solution and were uniformly dispersed by ball milling overnight. The mixture was further sonicated for 20 min to ensure complete homogeneity. The resulting polymer solution was fed through a capillary tip using a plastic syringe (10 ml). During electrospinning, a high voltage of 12 kV was applied to the needle, and the flow rate of the spinning solution was controlled to 0.5 ml h^{-1}. The distance between the tip and the rotating drum collector was 16 cm; the metal drum was rotated at 200 rpm. The electrospun fibers were collected on aluminum foil wrapped on the drum, and were dried in a vacuum oven at 60 °C for 12 h before further use. The thickness of the fibrous composite membrane was controlled to be about 25 μm.

2.3. Electrode preparation and cell assembly

Nanocrystalline TiO_2 paste was cast onto fluorine-doped tin oxide glass using a doctor blade and was sintered at 450 °C for 30 min. Its thickness was optimized at 12 μm, and it was sensitized overnight with a 0.3 mM solution of N719 dye in acetonitrile and tert-butyl alcohol (1:1 volume ratio) at room temperature. The counter electrode was prepared by spin-coating a 0.01 M solution of H_2PtCl_6 in isopropanol onto the fluorine-doped tin oxide glass and sintering at 450 °C for 30 min. A dye-sensitized solar cell was fabricated by sandwiching the fibrous composite membrane between a dye-coated TiO_2 electrode and a platinum counter electrode, and heat-sealing the perimeter of the cell while pressurizing it. A liquid electrolyte was then injected into the cell through the holes on the counter electrode. The liquid electrolyte was composed of 0.5 M LiI, 0.05 M I_2 and 0.05 M TBP dissolved in acetonitrile. Upon injection of liquid electrolyte, the gelation of membrane occurred and the liquid electrolyte was well trapped in the membrane. The holes in the counter electrode that were used to inject the electrolyte were then sealed by a sealant.

2.4. Characterization and measurements

Morphologies of electrospun PAN and PAN/silica fibrous membranes were examined using a field emission scanning electron microscope (FE-SEM, JEOL JSM-6300). The elemental distribution of Si in the PAN/silica fibrous membranes was examined using energy dispersive X-ray spectroscopy (EDX). Fourier transform infrared (FT-IR) spectra were recorded on a Magna IR 760 spectrometer in the range of 400-4000 cm^{-1} using pressed pellets of KBr powder. Differential scanning calorimetry (DSC) measurements were carried out at a heating rate of 10 °C min^{-1} in the temperature range of 25 to 200 °C. The porosity of the fibrous membranes was measured by the n-butanol uptake method [30]. In order to measure the electrolyte uptake and ionic conductivity, the electrospun membrane was immersed in liquid electrolyte for 1 h. The uptake of the electrolyte solution was then determined by using equation (1):

$$\text{uptake}\,(\%) = (M_{wet}\,M_{dry})/M_{dry} \times 100, \quad (1)$$

where M_{dry} and M_{wet} are the weights of the membrane before and after soaking in the liquid electrolyte, respectively [31,32]. For conductivity measurements, the membranes soaked with liquid electrolyte were sandwiched between two stainless steel electrodes. AC impedance measurements were then performed to measure the ionic conductivity using a Zahner Electrik IM6 impedance analyzer over the frequency range of 10 Hz to 100 kHz with amplitude of 10 mV. A two-electrode electrochemical cell consisting of a wetted membrane sandwiched with two identical Pt electrodes was used to make diffusion-limited current measurements, from which the diffusion coefficient of the triiodide ion was calculated. [33,34]. The diffusion-limited current was determined by cyclic voltammetry using a scan rate of 5 mV s^{-1}. Tafel polarization curves were obtained with different fibrous composite membranes using symmetric Pt cells in the potential range of ±1 V. The photovoltaic performance of the DSSCs was evaluated using a Xe light source (100 $mWcm^{-2}$) with an AM 1.5 filter in a solar simulator at ambient temperature. Light intensity was calibrated using a NREL-calibrated Si solar cell (PV Measurements, Inc.). A black mask with an aperture of 0.25 cm^2 was placed over the cells during irradiation, and an anti-reflection glass was placed on the front glass cover of the cells. AC impedance measurements of DSSCs were performed using an impedance analyzer over a frequency range of 10 mHz to 100 kHz at open circuit under 1 Sun illumination.

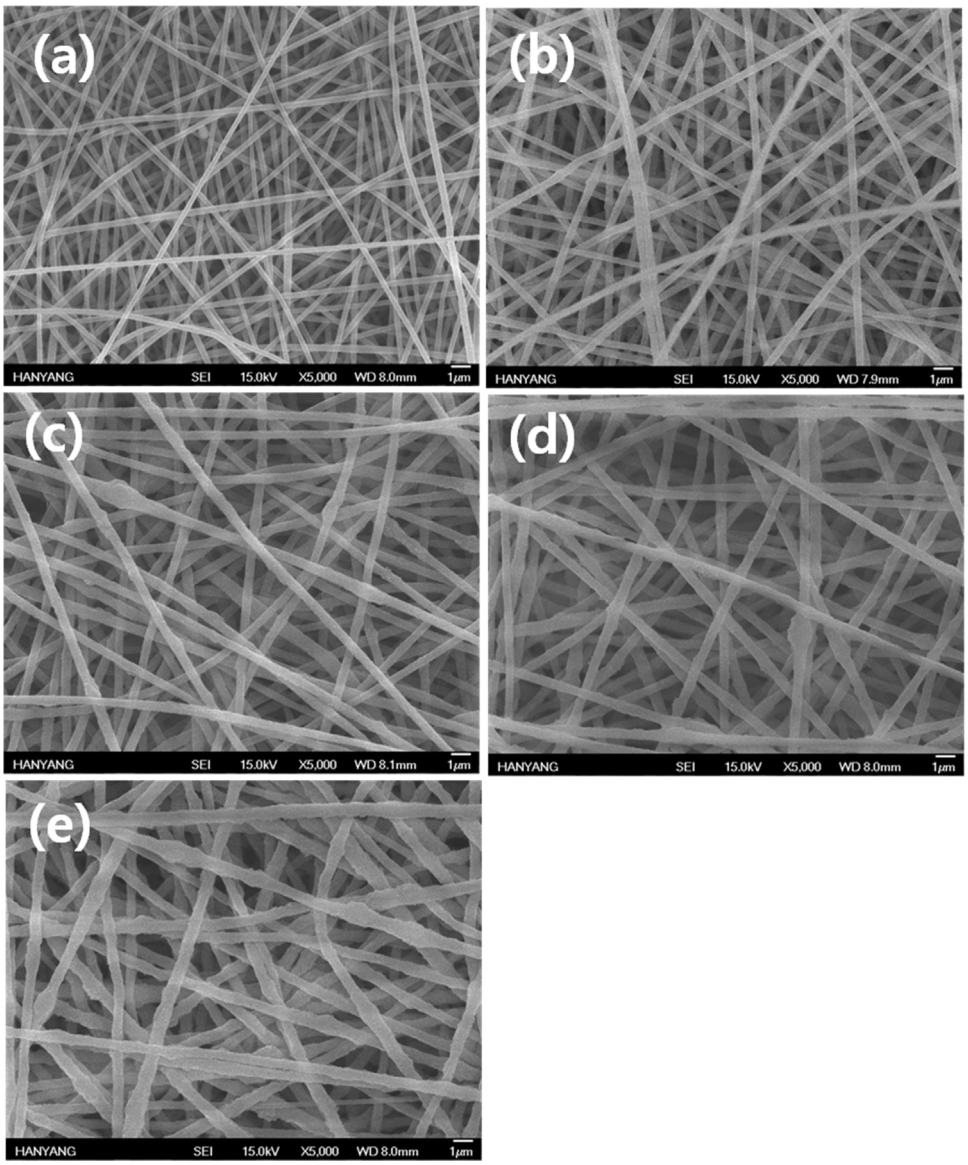

Fig. 2. FE-SEM images of electrospun PAN membranes containing various contents of SiO_2 particles: (a) 0 wt.% (i.e., pure PAN), (b) 5 wt.%, (c) 10 wt.%, (d) 15 wt.%, (e) 20 wt.%.

3. Results and discussion

Fig. 2 shows the SEM images of the electrospun PAN and PAN/SiO_2 fibrous composite membranes with various SiO_2 contents. As shown in figure, all the electrospun membranes had a highly porous three-dimensional fibrous interconnected network structure in which the SiO_2 nanoparticles are embedded. Thus, they are expected to be capable of the uptake of a large amount of electrolyte solution in their pores. The PAN membrane without SiO_2 exhibited a comparatively uniform morphology with an average fiber diameter of 290 nm. Both fiber diameter and surface roughness were observed to increase with SiO_2 content. The formation of larger-diameter fibers can be attributed to the substantial increase in viscosity of the polymer solution resulting from the addition of SiO_2 particles. The high viscosity of the electrospinning solution leads to the ejection of a larger fluid jet from the needle, which consequently forms thicker fibers [35].

Fig. 3 shows the EDX mapping images of Si in the electrospun PAN/SiO_2 fibrous composite membranes containing various contents of SiO_2 nanoparticles. As expected, the Si content increases with the content of SiO_2 particles. The SiO_2 particles are observed to be homogeneously distributed in the electrospun composite membrane without agglomeration, even for formulations with high SiO_2 content. It is plausible that SiOH in the fumed silica has a high affinity with the–CN groups in PAN. In this case, the hydrogen bonding between SiO_2 particles and PAN would produce a reinforcing interfacial interaction between the two phases, resulting in the homogeneous silica dispersion.

Fig. 4 shows FT-IR spectra of the electrospun PAN and PAN/SiO_2 composite membranes with various SiO_2 contents. The spectrum of the pure PAN membrane reveals characteristic peaks of PAN at 2930, 2240 and 1470 cm^{-1}, which respectively correspond to the stretching vibration of methylene (–CH_2–), the stretching vibration of nitrile groups (–CN), and the bending vibration of methylene [36]. It can be seen that the relative intensities of the peaks around 1100 cm^{-1} increased with the SiO_2 content; these peaks can be ascribed to the characteristic Si–O–Si asymmetric stretching vibration [37–39]. A broad peak near 3746 cm^{-1} was observed, corresponding to the characteristic band of–OH groups in the SiO_2 particles. This peak is associated with stretching vibrations involving these hydroxyl groups which result from hydrogen bonds of the Si–OH [40]. To investigate the effect of SiO_2 content on the

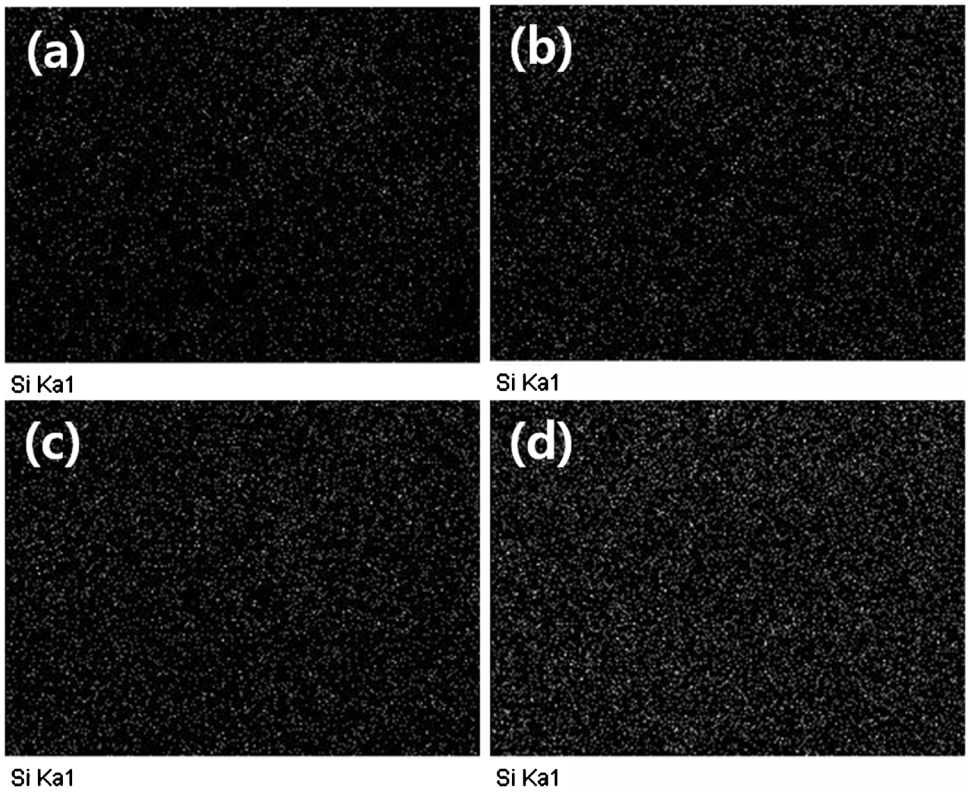

Fig. 3. EDX mapping images of Si in the electrospun PAN/SiO_2 composite membranes containing various contents of SiO_2 particles: (a) 5 wt.% (b) 10 wt.%, (c) 15 wt.%, (d) 20 wt.%.

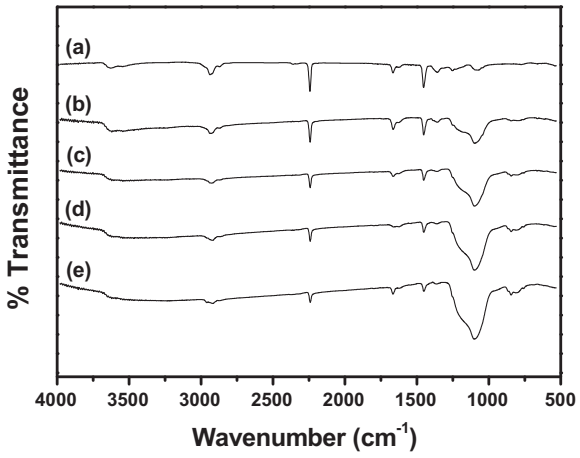

Fig. 4. FT-IR spectra of electrospun PAN membranes containing various contents of SiO_2 particles: (a) 0 wt.% (i.e., pure PAN), (b) 5 wt.%, (c) 10 wt.%, (d) 15 wt.%, (e) 20 wt.%.

interaction between the PAN and the silica particles, the glass temperatures (T_g) of the electrospun PAN and PAN/SiO_2 composite membranes were measured. The PAN membrane exhibited a T_g of 113.2 °C, and adding SiO_2 progressively increased T_g: the PAN/SiO_2 composite membranes of 5, 10, 15, 20 wt.% SiO_2 had respective T_g of 115.2, 116.3, 118.9 and 121.1 °C. This result suggests that the intermolecular interactions occurred between PAN and the SiO_2 particles, which reduced the cooperative segmental mobility of the polymer chains.

Fig. 5-(a) shows the porosity and electrolyte uptake of the electrospun PAN and PAN/SiO_2 fibrous composite membranes, as a function of SiO_2 content. All the electrospun membranes had high porosities exceeding 80.3%, due to the well-developed interstices

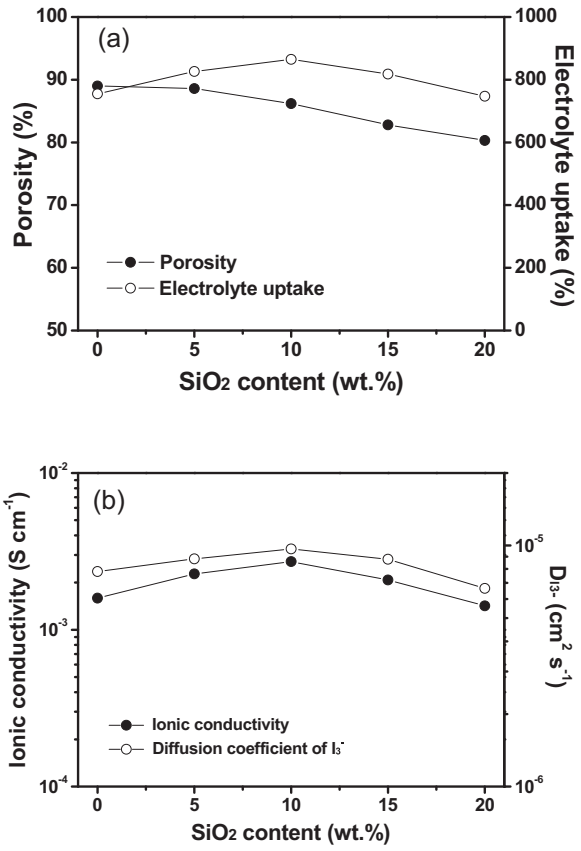

Fig. 5. Effects of SiO_2 content in the electrospun PAN/SiO_2 fibrous composite membranes on (a) porosity and electrolyte uptake and (b) ionic conductivity and diffusion coefficient of I_3^-.

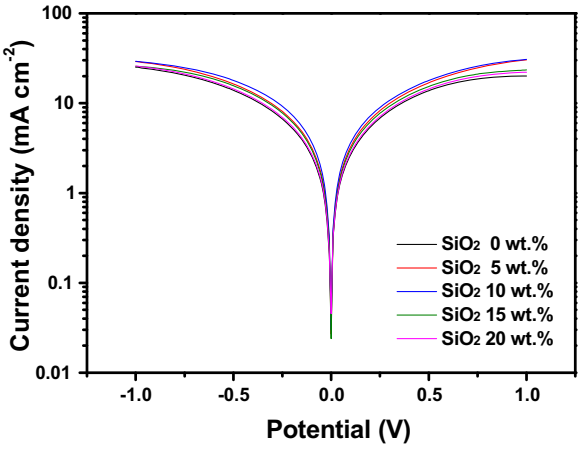

Fig. 6. Tafel polarization curves of symmetric Pt cells with electrospun PAN and PAN/SiO_2 composite membranes containing different contents of SiO_2.

formed by the interweaving of fibers, as shown in Fig. 2. The porosity gradually decreased from 89.0 to 80.3% as the SiO_2 content was increased from 0 to 20 wt.%. When the electrospun PAN and PAN/SiO_2 composite membranes were soaked in liquid electrolyte, the electrolyte uptake increased as the SiO_2 content was increased from 0 to 10 wt.%, and then decreased with further increase in SiO_2 content. The initial increase in electrolyte uptake with the addition of SiO_2 was related to the enhancement of the solution retention capacity, that is, the ability to hold liquid electrolyte. As previously reported [41], the hydrophilicity of SiO_2 nanoparticles gives them a high absorption capability and consequently enables loading of the polar organic solvent. The decrease in electrolyte uptake beyond 10 wt.% can be attributed the decrease of porosity with further addition of SiO_2. Jung et al. also reported that the electrolyte uptake reached a maximum at the 12 wt.% SiO_2 composition of a PAN/SiO_2 composite membrane for lithium battery applications [42]. Fig. 5-(b) shows the ionic conductivities and I_3^- diffusion coefficients in the PAN/SiO_2 electrospun fibrous membrane electrolytes as a function of SiO_2 content. Both the ionic conductivities and diffusion coefficients initially increase with increasing content of SiO_2 particles, reaching a maximum at 10 wt.% and decreasing after that point. The increase in ionic conductivity and diffusion coefficient promoted by the SiO_2 particles is associated with enhanced electrolyte uptake, as shown in Fig. 5-(a). In addition, introducing Lewis acid-base interactions between the surface silanol groups of the SiO_2 particles and the lithium ions immobilizes the cations, promoting efficient anionic (I_3^-) transport [43]. The decrease in ionic conductivity and diffusion coefficient observed for formulations with SiO_2 content greater than 10 wt.% may arise from both declining electrolyte uptake and a blocking effect on charge carrier transport of the electrically insulating SiO_2 particles [32]. At the optimum 10 wt.% SiO_2, the ionic conductivity and the diffusion coefficient of I_3^- are 2.7×10^{-3} S cm^{-1} and 9.5×10^{-6} cm^2 s^{-1}, respectively.

Before comparing the photovoltaic performance of the DSSCs with different fibrous composite membranes, Tafel polarization curves were obtained using symmetric Pt cells with different composite membranes in the potential range of -1.0 to 1.0 V, as shown in Fig. 6. The exchange current densities (j_o) for the electrochemical reaction ($I_3^- + 2e^- \leftrightarrow 3I^-$) were calculated from the intersection of linear anodic and cathodic curves. As a result, the cells with PAN/SiO_2 composite membranes of 0, 5, 10, 15, 20 wt.% SiO_2 exhibited respective j_o of 5.51, 6.38, 7.35, 6.36 and 5.68 mA cm^{-2}, indicating a facile redox reaction in the composite polymer electrolytes containing SiO_2 nanoparticles.

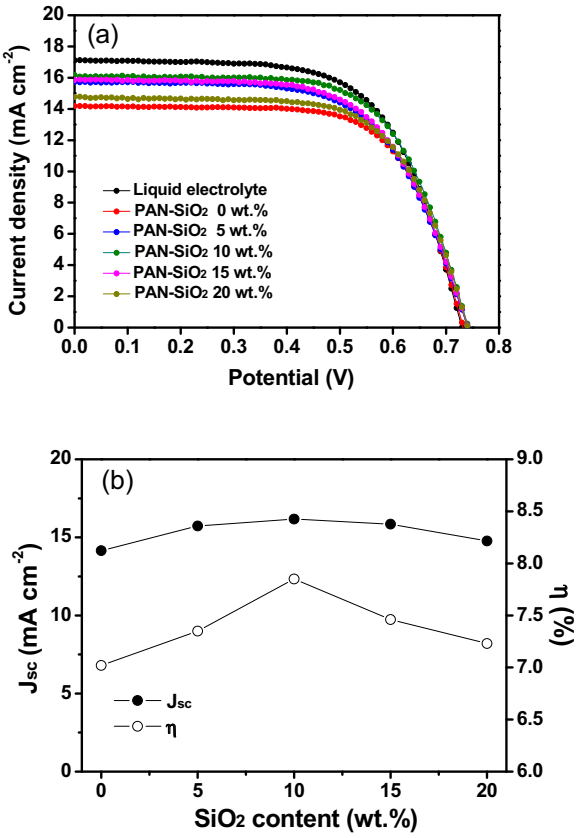

Fig. 7. Effects of SiO_2 content in the electrospun PAN/SiO_2 fibrous composite membranes on the photovoltaic performances of DSSCs assembled with these membranes: (a) DSSC photocurrent-voltage curves and (b) J_{sc} and η *vs.* SiO_2 content.

The photovoltaic performance of DSSCs assembled with electrospun PAN and PAN/SiO_2 composite membranes was evaluated, and the results are shown in Fig. 7. The addition of SiO_2 particles appeared to have a very minor influence on V_{oc}. On the other hand, the short-circuit current density (J_{sc}) and conversion efficiency (η) of the DSSCs increased with increasing the SiO_2 content up to 10 wt.%, decreasing with further addition. These results are related to improved diffusion of I_3^- at 10 wt.% SiO_2, as explained above in reference to the results in Fig. 5-(b). Thus, the optimum SiO_2 content to achieve the highest conversion efficiency is about 10 wt.%. Notably, the conversion efficiency (7.85%) of the DSSC assembled with the electrospun PAN/SiO_2 fibrous composite membrane containing 10 wt.% SiO_2 was comparable to that of a DSSC based on liquid electrolyte (8.02%). To our knowledge, the conversion efficiency of the DSSC assembled herein using a PAN/SiO_2 electrospun fibrous composite membrane was higher than those of DSSCs with PAN-based gel polymer electrolytes reported so far [11,24–28].

In order to investigate the effect of SiO_2 content on the impedance behavior of the DSSCs, the AC impedance measurements of the cells were performed. The resulting AC impedance spectra of DSSCs with electrospun PAN and PAN/SiO_2 composite membranes containing different contents of SiO_2 are compared in Fig. 8. As shown, the spectra exhibit three overlapping semicircles, which can be assigned to the electrochemical reaction at the counter Pt electrode (R_{ct1}), the charge transfer reaction at the TiO_2 electrode (R_{ct2}), and the Warburg diffusion of I^-/I_3^- (R_{diff}), respectively [44,45]. The electrolyte resistance (R_e) can be estimated from the intercept on the real axis in the high frequency range. It is found that the cell with composite PAN membrane containing 10 wt.% SiO_2 exhibits the lowest electrolyte resistance (R_e) and interfacial resistances (R_{ct1} and R_{ct2}). This result indicates that the addition

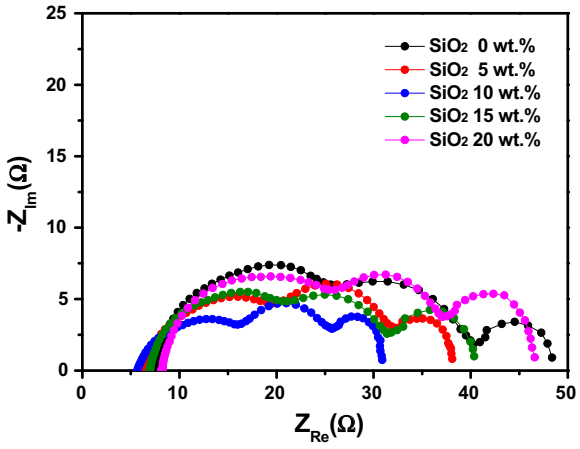

Fig. 8. AC impedance spectra of DSSCs with electrospun PAN and PAN/SiO_2 composite membranes containing different contents of SiO_2.

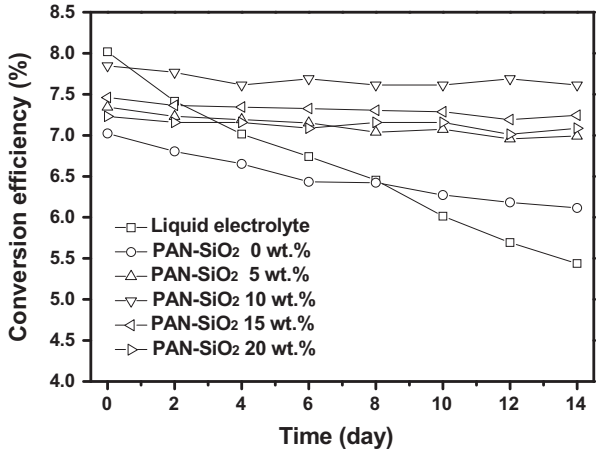

Fig. 9. Variation of conversion efficiency as a function of time for the DSSCs assembled with liquid electrolyte and electrospun PAN/SiO_2 fibrous composite membranes containing different content of SiO_2 particles.

of an appropriate amount of SiO_2 not only reduces the electrolyte resistance but also improves the charge transfer reaction at both TiO_2 electrode and counter electrode, resulting in the highest conversion efficiency in the DSSC with PAN/SiO_2 composite membrane containing 10 wt.% SiO_2.

The long-term stability of the DSSCs with electrospun fibrous membranes was evaluated. Fig. 9 represents the variation of conversion efficiency of the DSSCs as a function of time. For comparison, the conversion efficiency of the DSSC with liquid electrolyte is also shown. The conversion efficiency of the DSSC based on liquid electrolyte decayed continuously during the period of investigation; this gradual decrease was related to the evaporation of liquid electrolyte. On the other hand, the cells assembled with PAN/SiO_2 electrospun fibrous membranes exhibited fairly stable performance. The conversion efficiency that these cells retained after 14 days was improved from 87.1 to 98.0% as the SiO_2 content was increased from 0 to 20 wt.%. The improved stability of the cell assembled with the electrospun fibrous membrane containing a high content of SiO_2 particle was due to the fact that the organic solvent containing the I^-/I_3^- redox couple was well encapsulated in the cell, because SiO_2 nanoparticles and PAN polymer matrix helped to absorb the electrolyte, thereby preventing leakage of the electrolyte solution. The adhesive nature of polymer electrolytes also promoted favorable interfacial contact between the dye-adsorbed TiO_2 electrode and the Pt counter electrode, providing more stable performance than the DSSC assembled with liquid electrolyte.

4. Conclusions

PAN/SiO_2 electrospun composite fibrous membranes containing various amounts of SiO_2 nanoparticles were prepared and characterized. The fibrous composite membranes encapsulated a large amount of electrolyte solution, and thus exhibited high ionic conductivities that allowed their application in DSSCs. The addition of SiO_2 not only reduced the electrolyte resistance but also improved the charge transfer reaction at both TiO_2 electrode and counter electrode, resulting in the improved conversion efficiency of DSSCs made from the electrospun composite membranes. The DSSC assembled with the fibrous composite membrane containing 10 wt.% SiO_2 particles exhibited the remarkably high conversion efficiency of 7.85% at 100 mW cm^{-2}, and had better long-term stability than the DSSC assembled with liquid electrolyte.

Acknowledgements

This work was supported by the National Research Foundation of Korea (NRF) grant funded by the Korea government (MSIP) for the Center for Next Generation Dye-sensitized Solar Cells (No. 2008-0061903), and by a grant of the Human Resources Development Program of KETEP, funded by the Ministry of Trade, Industry and Energy of Korea (No. 20124010203290).

References

[1] B. O'Reagen, M. Gratzel, A low-cost, high-efficiency solar-cell based on dye-sensitized colloidal TiO_2 Films, Nature 353 (1991) 737–740.
[2] M. Gratzel, Photoelectrochemical cells, Nature 414 (2001) 338–344.
[3] A. Yella, H.W. Lee, H.N. Tsao, C.Y. Yi, A.K. Chandiran, M.K. Nazeeruddin, E.W.G. Diau, C.Y. Yeh, S.M. Zakeeruddin, M. Gratzel, Porphyrin-sensitized solar cells with cobalt (II/III)-based redox electrolyte exceed 12 percent efficiency, Science 334 (2011) 629–634.
[4] Y. Wang, Recent research progress on polymer electrolytes for dye-sensitized solar cells, Sol. Energy Mater. Sol. Cells 93 (2009) 1167–1175.
[5] P. Wang, S.M. Zakeeruddin, J.E. Moser, M.K. Nazeeruddin, T. Sekiguchi, M. Gratzel, A stable quasi-solid-state dye-sensitized solar cell with an amphiphilic ruthenium sensitizer and polymer gel electrolyte, Nat. Mater. 2 (2003) 402–407.
[6] J. Wu, Z. Lan, D. Wang, S. Hao, J. Lin, Y. Huang, S. Yin, T. Sato, Gel polymer electrolyte based on poly(acrylonitrile-*co*-styrene) and a novel organic iodide salt for quasi-solid state dye-sensitized solar cell, Electrochim. Acta 51 (2006) 4243–4249.
[7] V. Suryanarayanan, K.M. Lee, W.H. Ho, H.C. Chen, K.C. Ho, A comparative study of gel polymer electrolytes based on PVDF-HFP and liquid electrolytes containing imidazolinium ionic liquids of different carbon chain lengths in DSSCs, Sol. Energy Mater. Sol. Cells 91 (2007) 1467–1471.
[8] S.J. Lim, Y.S. Kang, D.W. Kim, Dye-sensitized solar cells with quasi-solid-state cross-linked polymer electrolytes containing aluminum oxide, Electrochim. Acta 56 (2011) 2031–2035.
[9] M. Wang, X. Pan, X.Q. Fang, L. Guo, C.N. Zhang, Y. Huang, Z.P. Huo, S.Y. Dai, Liquid crystal based electrolyte with light trapping scheme for enhancing photovoltaic performance of quasi-solid-state dye-sensitized solar cells, J. Power Sources 196 (2011) 5784–5791.
[10] J.Y. Song, Y.Y. Wang, C.C. Wan, Review of gel-type polymer electrolytes for lithium-ion batteries, J. Power Sources 77 (1999) 183–197.
[11] D.W. Kim, Y.B. Jeong, S.H. Kim, D.Y. Lee, J.S. Song, Photovoltaic performance of dye-sensitized solar cell assembled with gel polymer electrolyte, J. Power Sources 149 (2005) 112–116.
[12] A.R.S. Priya, A. Subramania, Y.S. Jung, K.J. Kim, High-performance quasi-solid-state dye-sensitized solar cell based on an electrospun PVdF-HFP membrane electrolyte, Langmuir 24 (2008) 9816–9819.
[13] S. Peng, L. Li, H. Tan, M. Srinivasan, S.G. Mhaisalkar, S. Ramakrishna, Q. Yan, Platinum/polyaniline transparent counter electrodes for quasi-solid dye-sensitized solar cells with electrospun PVDF-HFP/TiO_2 membrane electrolyte, Electrochim. Acta 105 (2013) 447–454.
[14] J.U. Kim, S.H. Park, H.J. Choi, W.K. Lee, J.K. Lee, M.R. Kim, Effect of electrolyte in electrospun poly(vinylidene fluoride-co-hexafluoropropylene) nanofibers on dye-sensitized solar cells, Sol. Energy Mater. Sol. Cells 93 (2009) 803–807.

[15] S.K. Ahn, T. Ban, P. Sakthivel, J.W. Lee, Y.S. Gal, J.K. Lee, M.R. Kim, S.H. Jin, Development of dye-densitized solar cells composed of liquid crystal embedded, electrospun poly(vinylidene fluoride-co-hexafluoropropylene) nanofibers as polymer gel electrolytes, ACS Appl. Mater. Interfaces 4 (2012) 2096–2100.
[16] M. Sethupathy, P. Pandey, P. Manisankar, Photovoltaic performance of dye-sensitized solar cells fabricated with polyvinylidene fluoride–polyacrylonitrile–silicondioxide hybrid composite membrane, Mater. Chem. Phys. 143 (2014) 1191–1198.
[17] C.R. Martin, Membrane-based synthesis of nanomaterials, Chem. Mater. 8 (1996) 1739–1746.
[18] D.W. Kim, Y.K. Sun, Electrochemical characterization of gel polymer electrolytes prepared with porous membranes, J. Power Sources 102 (2001) 41–45.
[19] L. Feng, S. Li, H. Li, J. Zhai, Y. Song, L. Jiang, Super-hydrophobic surface of aligned polyacrylonitrile nanofibers, Angew. Chem. Int. Ed. 41 (2002) 1221–1223.
[20] J.K. Kim, G. Cheruvally, X. Li, J.H. Ahn, K.W. Kim, H.J. Ahn, Preparation and electrochemical characterization of electrospun, microporous membrane-based composite polymer electrolytes for lithium batteries, J. Power Sources 178 (2008) 815–820.
[21] H.R. Jung, W.J. Lee, Electrochemical characteristics of electrospun poly(methyl methacrylate)/polyvinyl chloride as gel polymer electrolytes for lithium ion battery, Electrochim. Acta 58 (2011) 674–680.
[22] F. Liu, N.A. Hashim, Y. Liu, M.R.M. Abed, K. Li, Progress in the production and modification of PVDF membranes, J. Membr. Sci. 375 (2011) 1–27.
[23] N. Shubha, R. Prasanth, H.H. Hoon, M. Srinivasan, Plastic crystalline-semi crystalline polymer composite electrolyte based on non-woven poly(vinylidenefluoride-co-hexafluoropropylene) porous membranes for lithium ion batteries, Electrochim. Acta 125 (2014) 362–370.
[24] O.A. Ileperuma, M.A.K.L. Dissanayake, S. Somasundaram, Dye-sensitised photoelectrochemical solar cells with polyacrylonitrile based solid polymer electrolytes, Electrochim. Acta 47 (2002) 2801–2807.
[25] T.M.W.J. Bandara, M.A.K.L. Dissanayake, B.-E. Mellander, Dye sensitized solar cells with poly(acrylonitrile) based plasticized electrolyte containing MgI_2, Electrochim. Acta 55 (2010) 2044–2047.
[26] O.A. Ileperuma, G.R.A. Kumara, H.-S. Yang, K. Murakami, Quasi-solid electrolyte based on polyacrylonitrile for dye-sensitized solar cells, J. Photochem. Photobiol. A 217 (2011) 308–312.
[27] Y.F. Chan, C.C. Wang, C.Y. Chen, Quasi-solid DSSC based on a gel-state electrolyte of PAN with 2-D graphenes incorporated, J. Mater. Chem. A 1 (2013) 5479–5486.
[28] M.A.K.L. Dissanayake, C.A. Thotawatthage, G.K.R. Senadeera, T.M.W.J. Bandara, W.J.M.J.S.R. Jayasundera, B.E. Mellander, Efficiency enhancement by mixed cation effect in dye-sensitized solar cells with PAN based gel polymer electrolyte, J. Photochem. Photobiol. A 246 (2012) 29–35.
[29] F. Croce, G.B. Appetecchi, L. Persi, B. Scrosati, Nanocomposite polymer electrolytes for lithium batteries, Nature 394 (1998) 456–458.
[30] S.W. Choi, J.R. Kim, S.M. Jo, W.S. Lee, Y.R. Kim, Electrochemical and spectroscopic properties of electrospun PAN-based fibrous polymer electrolytes, J. Electrochem. Soc. 152 (2005) A989–A995.
[31] Y. Ding, P. Zhang, Z. Long, Y. Jiang, F. Xu, W. Di, The ionic conductivity and mechanical property of electrospun P(VdF-HFP)/PMMA membranes for lithium ion batteries, J. Membr. Sci. 329 (2009) 56–59.
[32] W.K. Shin, D.W. Kim, High performance ceramic-coated separators prepared with lithium ion-containing SiO_2 particles for lithium-ion batteries, J. Power Sources 226 (2013) 54–60.
[33] A. Hauch, A. Georg, Diffusion in the electrolyte and charge-transfer reaction at the platinum electrode in dye-sensitized solar cells, Electrochim. Acta 46 (2001) 3457–3466.
[34] M. Zistler, P. Wachter, P. Wasserscheid, D. Gerhard, A. Hinsch, R. Sastrawan, H.J. Gores, Comparison of electrochemical methods for triiodide diffusion coefficient measurements and observation of non-Stokesian diffusion behavior in binary mixtures of two ionic liquids, Electrochim. Acta 52 (2006) 161–169.
[35] Z.M. Huang, Y.Z. Zhang, M. Kotaki, S. Ramakrishna, A review on polymer nanofibers by electrospinning and their applications in nanocomposites, Compos. Sci. Technol. 63 (2003) 2223–2253.
[36] Y. Wang, J. Liu, J.Y. Liang, Thermo-chemical reactions of modified PAN fibers during heat-treatment process, Adv. Mat. Res. 11 (2006) 73–76.
[37] B. Ding, H. Kim, C. Kim, M. Khil, S. Park, Morphology and crystalline phase study of electrospun TiO_2-SiO_2 nanofibres, Nanotechnology 14 (2003) 532–537.
[38] S.W. Lee, Y.U. Kim, S.S. Choi, T.Y. Park, Y.L. Joo, S.G. Lee, Preparation of SiO_2/TiO_2 composite fibers by sol-gel reaction and electrospinning, Mater. Lett. 61 (2007) 889–893.
[39] Y.S. Lee, S.H. Ju, J.H. Kim, S.S. Hwang, J.M. Choi, Y.K. Sun, H. Kim, B. Scrosati, D.W. Kim, Composite gel polymer electrolytes containing core-shell structured $SiO_2(Li^+)$ particles for lithium-ion polymer batteries, Electrochem. Commun. 17 (2012) 18–21.
[40] L. Ji, X. Zhang, Ultrafine polyacrylonitrile/silica composite fibers via electrospinning, Mat. Res. 62 (2008) 2161–2164.
[41] D.W. Kim, Y.K. Sun, Polymer electrolytes based on acrylonitrile-methyl methacrylate-styrene terpolymers for rechargeable lithium polymer batteries, J. Electrochem. Soc. 145 (1998) 1958–1963.
[42] H.R. Jung, D.H. Ju, W.J. Lee, X. Zhang, R. Kotek, Electrospun hydrophilic fumed silica/polyacrylonitrile nanofiber-based composite electrolyte membranes, Electrochim. Acta 54 (2009) 3630–3637.
[43] P. Raghaven, J.W. Choi, J.H. Ahn, G. Cheruvally, G.S. Chauhan, H.J. Ahn, C. Nah, Novel electrospun poly(vinylidene fluoride-co-hexafluoropropylene)-in situ SiO_2 composite membrane-based polymer electrolyte for lithium batteries, J Power Sources 184 (2008) 437–443.
[44] C. Longo, J. Freitas, M.A. De Paoli, Performance and stability of TiO_2/dye solar cells assembled with flexible electrodes and a polymer electrolyte, J. Photochem. Photobiol. A: Chem. 159 (2003) 33–39.
[45] K.-M. Lee, V. Suryanarayanan, K.-C. Ho, A photo-physical and electrochemical impedance spectroscopy study on the quasi-solid state dye-sensitized solar cells based on poly(vinylidene fluoride-co-hexafluoropropylene), J. Power Sources 185 (2008) 1605–1612.